

The Cyborg Astrobiologist: scouting red beds for uncommon features with geological significance

Patrick Charles McGuire^{1*}, Enrique Díaz-Martínez^{2**}, Jens Ormö³, Javier Gómez-Elvira⁴, José Antonio Rodríguez-Manfredi⁴, Eduardo Sebastián-Martínez⁴, Helge Ritter⁵, Robert Haschke⁵, Markus Oesker⁵ and Jörg Ontrup⁵

¹Robotics & Planetary Exploration Laboratory, and Transdisciplinary Laboratory, Centro de Astrobiología (INTA/CSIC), Instituto Nacional Técnica Aeroespacial, Carretera de Torrejón a Ajalvir km 4.5, Torrejón de Ardoz, Madrid, Spain 28850

e-mail: mcguire@physik.uni-bielefeld.de

²Dirección de Geología y Geofísica, Instituto Geológico y Minero de España, Calera 1, Tres Cantos, Madrid, Spain 28760

³Planetary Geology Laboratory, Centro de Astrobiología (INTA/CSIC), Instituto Nacional Técnica Aeroespacial, Carretera de Torrejón a Ajalvir km 4.5, Torrejón de Ardoz, Madrid, Spain 28850

⁴Robotics & Planetary Exploration Laboratory, Centro de Astrobiología (INTA/CSIC), Instituto Nacional Técnica Aeroespacial, Carretera de Torrejón a Ajalvir km 4.5, Torrejón de Ardoz, Madrid, Spain 28850

⁵Neuroinformatics Group, Computer Science Department, Technische Fakultät, University of Bielefeld, PO Box 10 01 31, Bielefeld, Germany 33501

Abstract: The ‘Cyborg Astrobiologist’ has undergone a second geological field trial, at a site in northern Guadalajara, Spain, near Riba de Santiuste. The site at Riba de Santiuste is dominated by layered deposits of red sandstones. The Cyborg Astrobiologist is a wearable computer and video camera system that has demonstrated a capability to find uncommon interest points in geological imagery in real time in the field. In this second field trial, the computer vision system of the Cyborg Astrobiologist was tested at seven different tripod positions, on three different geological structures. The first geological structure was an outcrop of nearly homogeneous sandstone, which exhibits oxidized-iron impurities in red areas and an absence of these iron impurities in white areas. The white areas in these ‘red beds’ have turned white because the iron has been removed. The iron removal from the sandstone can proceed once the iron has been chemically reduced, perhaps by a biological agent. In one instance the computer vision system found several (iron-free) white spots to be uncommon and therefore interesting, as well as several small and dark nodules. The second geological structure was another outcrop some 600 m to the east, with white, textured mineral deposits on the surface of the sandstone, at the bottom of the outcrop. The computer vision system found these white, textured mineral deposits to be interesting. We acquired samples of the mineral deposits for geochemical analysis in the laboratory. This laboratory analysis of the crust identifies a double layer, consisting of an internal millimetre-size layering of calcite and an external centimetre-size efflorescence of gypsum. The third geological structure was a 50 cm thick palaeosol layer, with fossilized root structures of some plants. The computer vision system also found certain areas of these root structures to be interesting. A quasi-blind comparison of the Cyborg Astrobiologist’s interest points for these images with the interest points determined afterwards by a human geologist shows that the Cyborg Astrobiologist concurred with the human geologist 68 % of the time (true-positive rate), with a 32 % false-positive rate and a 32 % false-negative rate. The performance of the Cyborg Astrobiologist’s computer vision system was by no means perfect, so there is plenty of room for improvement. However, these tests validate the image-segmentation and uncommon-mapping technique that we first employed at a different geological site (Rivas Vaciamadrid) with somewhat different properties for the imagery.

Received 4 April 2005, accepted 20 May 2005

Key words: computer vision, robotics, image segmentation, uncommon map, interest map, field geology, Mars, Meridiani Planum, wearable computers, co-occurrence histograms, red beds, red sandstones, nodules, concretions, reduction spheroids, Triassic period.

* Corresponding author. Address after 3 October 2005: McDonnell Center for the Space Sciences, Department of Earth & Planetary Sciences, and the Department of Physics, Washington University, Campus Box 1169, 1 Brookings Drive, Saint Louis, MO 63130-4862, USA.

** Formerly at: Planetary Geology Laboratory, Centro de Astrobiología.

Introduction

Half a lifetime has passed since human astronauts directly explored another planetary body. Currently, two robotic geologists are exploring the surface of Mars, one scientific probe has just landed on Saturn's moon Titan and a number of orbiters are studying several of the planets and moons in our Solar System. Soon, we will be sending more robotic explorers to Mars, more science stations to orbit our planetary neighbours and perhaps new human explorers to the Moon. All of these exploration systems, human or robotic, semi-autonomous or remote-operated, could benefit from enhancements in their capabilities of scientific autonomy. Human astronaut explorers can benefit from enhanced scientific autonomy – astronauts with 'augmented-reality' visors could explore more efficiently and perhaps make more discoveries than astronauts who exclusively rely upon guidance from Earth-based scientists and engineers. Remote-operated robotic rovers can benefit from enhanced scientific autonomy – this autonomy could either be on-board the rover¹ or in computers on Earth.² Such scientific autonomy can enhance the scientific productivity of these expensive missions, but only if the autonomy measures are well tested and therefore 'trustable' by the controllers on Earth.

Along these lines, we have constructed a field-capable platform (at relatively low cost) in order to develop and to test computer vision algorithms for space exploration here on Earth, prior to deployment in a space mission. This platform uses a wearable computer and a video camera,³ as well as the human operator (see Figure 1). Since this astrobiological exploration system is part human and part machine, we call our system the 'Cyborg Astrobiologist'.⁴ Recently, we have reported our first results at a geological field site with the Cyborg Astrobiologist exploration system (McGuire *et al.* 2004b). In this paper, we discuss our results at a second geological field site, near Riba de Santiuste, in northern Guadalajara, Spain (see the maps in Figs 2 and 3). This second geological field site offers a different type of imagery compared with that studied in the previous paper. This new imagery resembles some aspects of the imagery that Mars Exploration Rover (MER) Opportunity is currently studying on Mars, and the new imagery has greater astrobiological implications than the imagery studied in the previous mission of the Cyborg Astrobiologist. We show that the basic exploration algorithms that we introduced in our first paper also function rather well at this second field site, despite the change in the nature of the imagery.

¹ In the form of 'macros' or callable subroutines.

² In order to assist the night-time mission planners.

³ We are currently working towards extending these capabilities with the addition of a microscopic imager. In the future, we could also integrate near-infrared or mid-infrared spectrometers into the system, and perhaps a Raman spectrometer. For example, a thermal-emission spectrometer (TES) would be useful for identifying minerals in the field.

⁴ The word 'cyborg' is derived from 'cybernetic organism'.



Fig. 1. Ormõ with the Cyborg Astrobiologist system at tripod position 2, near outcrop 1 outside of Riba de Santiuste in the northern part of the Guadalajara province in central Spain. Díaz-Martínez is assisting; he is trying to identify the positions of the computer-determined interest points on the outcrop, which are annotated on the tablet display of the wearable computer. The image was segmented in real time, and we overlay the image segmentation (for saturation) on the red-sandstone outcrop. In Fig. 5, we present details of the determination of the interest map and the interest points for the image acquired and processed at this tripod position. This documents the Riba mission at 1:53 pm on 8 February 2004.

To give context to our work, we would like to remind the reader of two discoveries by the Apollo 15 and 17 astronauts on the Moon in the early 1970s, namely of the 'Genesis Rock' and of 'orange soil' (Compton 1989). The Apollo 15 astronauts were 'astronauts trained to be geologists', and one of their missions was to find 'ancient' rocks, in order to obtain information as to how the Moon was formed. Given the 'bias' of their mission, and given significant 'scientific autonomy' by mission control on the second day of their mission at the Hadley–Appenines landing site, astronauts Scott and Irwin found an anorthosite.⁵ Scott and Irwin dubbed this specimen 'the Genesis rock', because it possibly recorded the time after the molten Moon's surface first cooled down, over 4 billion years ago. They initially found the Genesis rock to be interesting partly because their mission requirements and their focused geological training biased them to look for such crystalline types of rock.

This biased search during the Apollo 15 mission on the Moon is not unlike one mission requirement of the MER Opportunity Rover. One main objective for sending Opportunity to the Meridiani Planum site on Mars was to understand the Mars Odyssey orbiter's suggestion of abundant coarse-grained grey haematite at Meridiani. So the initial focus and bias of Opportunity's study of Meridiani was

⁵ Anorthosite has a calcium aluminium silicate composition, with a crystalline and 'plagioclase' form. A plagioclase is a rock that exhibits obliquely cleaving crystals.



Fig. 2. Map of the north-eastern part of central Spain, showing the current field site, Riba de Santiuste, and the previous field site, Rivas Vaciamadrid. The location of part of our team's research center, the Centro de Astrobiología, is also indicated. The horizontal extent of this map is about 520 km.



Fig. 3. Map of the vicinity of Riba de Santiuste, with road numbers indicated. The horizontal extent of this map is 100 km.

on determining the source and nature of the haematite, and based upon this bias, Opportunity and the Earth-based geologists and engineers have been highly successful in writing 'the story' about haematite at Meridiani (Chan *et al.* 2004; Squyres *et al.* 2004).

The Apollo 17 mission had one astronaut who had been trained to be a geologist (Cernan) and one geologist who had trained to be an astronaut (Schmitt). One of Schmitt's responsibilities (as geologist/astronaut) was to try to see if he could observe phenomena on the Moon which the previous astronaut/geologists had not seen. Another responsibility for both Cernan and Schmitt was to try to find signs of recent

volcanism, which was one reason their Taurus–Littrow landing site had been chosen, since it contained numerous craters of possible volcanic origin. Despite the bias of the mission towards volcanic geology, Schmitt discovered an unusual 'orange soil' on the rim of one crater, which he initially thought could be due to some unusual oxidative process. This orange soil later turned out to be composed of small orangish glass-like beads, probably of volcanic origin. As with the rest of Schmitt's geological observing on the Moon in which 'he based his decisions on taking samples on visually detectable differences or similarities' (Compton 1989), Schmitt (1987) found the orange soil interesting

because it was different from anything else he had seen on the Moon. From our point of view, since Schmitt was an expert geologist, he was able to go much beyond the naive mission goals and biases of looking for fresh signs of volcanism, to discover something else (orange soil), which at the time seemed unrelated to volcanism. In summary, we point to the Apollo 15 and 17 missions and the MER Opportunity mission as examples of the need to have both biased and unbiased techniques for scientific autonomy during space exploration missions.

It is rather difficult to make a system that can reliably detect signatures of interesting geological and biological phenomena (with an imager or with a spectrometer) in a general and biased manner. In this report, we describe the further testing of our *unbiased* 'Cyborg Astrobiologist' system.

In the next section, we discuss the hardware and software of our system, this is followed by summaries and results of the geological expeditions to Riba de Santiuste and we finish with a more general discussion and conclusions.

The Cyborg Geologist and Astrobiologist system

Our ongoing effort in the area of autonomous recognition of scientific targets of opportunity for field geology and field astrobiology is maturing. To date, we have developed and field-tested a 'Cyborg Astrobiologist' system (McGuire *et al.* 2004a,b) that now can:

- use human mobility to manoeuvre to and within a geological site;
- use a portable robotic camera system to obtain a mosaic of colour images;
- use a 'wearable' computer to search in real time for the most uncommon regions of these mosaic images;
- use the robotic camera system to repoint at several of the most uncommon areas of the mosaic images, in order to obtain much more detailed information about these 'interesting' uncommon areas;
- choose one of the interesting areas in the panorama for a closer approach; and
- repeat the process as often as desired, sometimes retracing a step of the geological approach.

In the *Mars Exploration Workshop* held in Madrid in November 2003, we demonstrated some of the early capabilities of our 'Cyborg' Geologist/Astrobiologist System (McGuire *et al.* 2004a). We have been using this cyborg system as a platform to develop computer vision algorithms for recognizing interesting geological and astrobiological features, and for testing these algorithms in the field here on Earth (McGuire *et al.* 2004b).

The half-human/half-machine 'cyborg' approach (see Fig. 1) uses human locomotion to take the computer vision algorithms into the field for teaching and testing, using a wearable computer. This is advantageous because we can therefore concentrate on developing the 'scientific' aspects for the autonomous discovery of features in the computer imagery, as opposed to the more 'engineering' aspects of

using computer vision to guide the locomotion of a robot through treacherous terrain. This means the development of the scientific vision system for the robot is effectively decoupled from the development of the locomotion system for the robot.

After the maturation of the computer vision algorithms, we hope to transplant these algorithms from the Cyborg computer to the on-board computer of a semi-autonomous robot that will be bound for Mars or one of the interesting moons in our Solar System. These algorithms could also work in analysing remote-sensing data from orbiter spacecraft.

Image segmentation, uncommon maps, interest maps and interest points

With human vision, a geologist, in an unbiased approach to an outcrop (or scene):

- first, tends to pay attention to those areas of a scene which are most unlike the other areas of the scene; and then,
- secondly, attempts to find the relation between the different areas of the scene, in order to understand the geological history of the outcrop.⁶

The first step in this prototypical thought process of a geologist was our motivation for inventing the concept of uncommon maps. See McGuire *et al.* (2004b) for an introduction to the concept of an uncommon map and our implementation of it. We have not yet attempted to solve the second step in this prototypical thought process of a geologist, but it is evident from the formulation of the second step that human geologists do not immediately ignore the common areas of the scene. Instead, human geologists catalogue the common areas and put them in the back of their minds for 'higher-level analysis of the scene', or in other words, for determining explanations for the relations of the uncommon areas of the scene with the common areas of the scene.

For example, a dark, linear feature transects a light-toned, delineated surface. At this specific scale, the dark feature is uncommon, an 'interest point', as it has a specific relation to the surrounding light-toned material. It can 'tell the story' of the outcrop. Continued study may show how it cuts the delineation of the light-toned material, most likely indicating a younger age. Coupled with a capacity for microscopic analysis, or even better, spectrographic analysis of the mineralogy, a continued study may show the dark feature to be of basaltic composition and the light-toned material to be of granitic composition. This data compared with the information stored in the mind of the geologist (knowledge) may lead to the interpretation of the outcrop as a foliated granite (gneiss) cut by a dolerite dyke.

Prior to implementing the 'uncommon map', the first step of the prototypical geologist's thought process, we needed a segmentation algorithm, in order to produce pixel-class maps to serve as input to the uncommon-map algorithm. We have

⁶ This concept can be compared to regular geological base-mapping.

implemented the classic co-occurrence histogram algorithm (Haralick *et al.* 1973; Haddon & Boyce 1990). For this work, we have not included texture information in the segmentation algorithm nor in the uncommon-map algorithm. Currently, each of the three bands of hue, saturation and intensity (*H, S, I*) colour information is segmented separately, and later merged in the interest map by summing three independent uncommon maps. In ongoing work, we are working to integrate simultaneous colour and texture image segmentation into the Cyborg Astrobiologist system (e.g. Freixenet *et al.* 2004).

The concept of an ‘uncommon map’ is our invention, though it indubitably has been invented independently by other authors, since it is somewhat useful.⁷ In our implementation, the uncommon-map algorithm takes the top eight pixel classes determined by the image-segmentation algorithm, and ranks each pixel class according to how many pixels there are in each class. The pixels in the pixel class with the greatest number of pixel members are labelled numerically as ‘common’, and the pixels in the pixel class with the least number of pixel members are labelled numerically as ‘uncommon’. The ‘uncommonness’ hence ranges from 1 for a common pixel to 8 for an uncommon pixel, and we can therefore construct an uncommon map given any image-segmentation map. Rare pixels that belong to a pixel class of 9 or greater are usually noise pixels in our tests thus far, and are currently ignored. In our work, we construct several uncommon maps from the colour image mosaic, and then we sum these uncommon maps together, in order to arrive at a final interest map.

For more details on our particular software techniques, especially on image segmentation and uncommon mapping, see McGuire *et al.* (2004b).

Hardware for the Cyborg Astrobiologist

For this mission to Riba, the non-human hardware of the Cyborg Astrobiologist system consisted of:

- a 667 MHz wearable computer (from ViA Computer Systems in Minnesota) with a ‘power-saving’ Transmeta ‘Crusoe’ CPU and 112 MB of physical memory;
- an indoor/outdoor sunlight-readable tablet display with stylus (from ViA Computer Systems);
- a SONY ‘Handycam’ colour video camera (model *DCR-TRV620E-PAL*); and
- a tripod for the camera.

⁷ Note in proofs: News reports in 2005 (i.e. Chemical guidebook may help Mars Rover track extraterrestrial life, <http://www.sciencedaily.com/releases/2005/05/050504180149.htm>) brought the work at Idaho National Laboratory to our attention, in which the Idaho researchers use a mass spectrometer in raster mode on a sample, in order to make an ‘image’, within which they search for uncommon areas. They also perform higher-level fuzzy-logic processing with a spectral identification inference engine (SIDIE) of these ‘hyperspectral images’ of mass spectra. They have capabilities to blast more deeply into their samples, autonomously, if their inference engine suggests that it would be useful. See Scott *et al.* (2003) and Scott & Tremblay (2002) for the status of their system as of a couple of years ago.

The SONY Handycam provides real-time imagery to the wearable computer via an IEEE1394/Firewire communication cable. The system as deployed to Riba used two independent batteries: one for the computer, and the other for the camera. The power-saving aspect of the wearable computer’s Crusoe processor is important because it extends battery life, meaning that the human does not need to carry spare batteries. A single lithium-ion battery for the wearable computer, which weighs about 1 kg, was sufficient for this 4 h mission. Likewise, a single lithium-ion battery (SONY model NP-F960, 38.8 W h) was sufficient for the SONY Handycam for the 4 h mission to Riba, despite frequent use of the power-hungry fold-out LCD display for the Handycam.

The main reason for using the tripod during the mission to Riba was that it allowed the user to repoint the camera or to zoom in on a feature in the previously analysed image. In the previous study at Rivas (McGuire *et al.* 2004b), mosaicking and automated repointing were part of the study, so the stable platform provided by the tripod was essential. We eliminated the pan–tilt unit from the mission to Riba because removing the extra bag containing a battery and communication and power cables for the pan–tilt unit improved the mobility of the Cyborg Astrobiologist system. Another reason for eliminating the pan–tilt unit from the system for the mission to Riba was that it saved time since there was less time spent waiting around for the mosaicking and repointing to be completed. The capacities of automated mosaicking and of automated repointing at interest points are, however, essential to the system in the long run, and will be re-introduced at a later stage when needed.⁸ During this mission, the Cyborg Astrobiologist system analysed 32 images from seven different tripod positions at three different outcrops over a 600 m distance and over a 4 h period. During the previous mission at Rivas, with the pan–tilt unit enabled, the Cyborg Astrobiologist system only analysed 24 mosaic images from three different tripod positions at one outcrop over a 300 m distance and over a 5 h period (see Table 1 and Fig. 4).

For this particular study, the mobility granted by the wearable computer was almost essential. Using a more powerful non-wearable computer could have restricted the mobility somewhat, and would have made it more difficult to study the third outcrop on the slopes of the castle-topped hill. The head-mounted display that we used during the Rivas mission (2004) was much brighter than the tablet display used

⁸ The pan–tilt unit was not absolutely essential for the Riba mission, but it could have been useful. The geologists had some troubles at Riba, when they wanted to use the results of the Cyborg Astrobiologist’s analysis of a wide-angle image in order to repoint the camera at an interest point, and then zoom in on it. At one point the geologists decided to have one geologist point with his hand at a desired location on the rather uniformly coloured sandstone outcrop, so that the other geologist who was controlling the pointing of the camera could find that feature in the camera view-finder and point at the interesting feature and zoom in on it (see Fig. 1). If we had had the pan–tilt unit with us, then this would have been much more automatic, as the repointing could have been under computer control.

Table 1. A description of some of the parameters of the missions to Rivas Vaciamadrid and to Riba de Santiuste (w = with, w/o = without)

Mission location	Mission date(s)	Mission mode	Geology
Rivas Vaciamadrid	3 March 2004 11 June 2004	w pan-tilt unit w mosaicking w automated repointing w/o zoom lens w head-mounted display	Gypsum cliffs Gypsum wetting Miocene age
Riba de Santiuste	8 February 2005	w/o pan-tilt unit w/o mosaicking w/o automated repointing w zoom lens (manual) w tablet display	'Red beds' Red sandstones Redox geochemistry Sulphate deposits Triassic age

Mission location	Setup time	Mission duration	Mission distance
Rivas Vaciamadrid	1 h	5 h	300 m (by foot)
Riba de Santiuste	0.5 h (w teaching)	4 h	600 m (by vehicle, and partly by foot)

Mission location	Outcrops studied	Tripod positions	Images analysed
Rivas Vaciamadrid	1	3	24
Riba de Santiuste	3	7	32

Mission location	Interest points w human-geologist concurrence	False-negative interest points	False-positive interest points
Rivas Vaciamadrid	–	–	–
Riba de Santiuste	69	32	32

during the Riba mission. Together with the thumb-operated finger mouse, the head-mounted display was more ergonomic during the mission to Rivas, than was the tablet display and stylus used during this Riba mission. However, the spatial resolution of the head-mounted display was somewhat less than that of the tablet display. During the Riba mission, we wanted to share and interpret the results interactively between the three investigators. This would have been much more difficult with the single-user head-mounted display than it was with the multi-viewer higher-resolution tablet display. So we used the tablet display during the mission to Riba, with the intention of switching to the head-mounted display later in the day.⁹

Software for the Cyborg Astrobiologist

The wearable computer processes the images acquired by the colour digital video camera to compute a map of 'interesting' areas. What the system determines as 'interest-

ing' is based on the 'uncommon' maps introduced earlier in this paper. It is the relation between uncommon and common that eventually can tell the geological history of the outcrop. The computations use two-dimensional histogramming for image segmentation (Haralick *et al.* 1973; Haddon & Boyce 1990). This image segmentation is computed independently for each of the hue, saturation and intensity (H, S, I) image planes, resulting in three different image-segmentation maps. These image-segmentation maps were used to compute 'uncommon' maps (one for each of the three (H, S, I) image-segmentation maps): each of the three resulting uncommon maps gives highest weight to those regions of smallest area for the respective (H, S, I) image planes. Finally, the three (H, S, I) uncommon maps are added together into an interest map, which is used by the Cyborg system in order to determine the top three interest points to report to the human operator. The image-processing algorithms and robotic system-control algorithms are all programmed using the graphical programming language, NEO/NST (Ritter *et al.* 1992, 2002). Using such a graphical programming language adds flexibility and ease of understanding to our Cyborg Astrobiologist project, which is by its nature largely a software project. We discuss some of the details of the software implementation in McGuire *et al.* (2004b).

⁹ The multi-viewer interactivity provided by the tablet display offered more to us than the brighter screen of the head-mounted display, so we used the tablet display for the entire mission to Riba. It would be useful to be able to switch rapidly between the tablet display and the head-mounted display, but our system remains incapable of this at this moment.

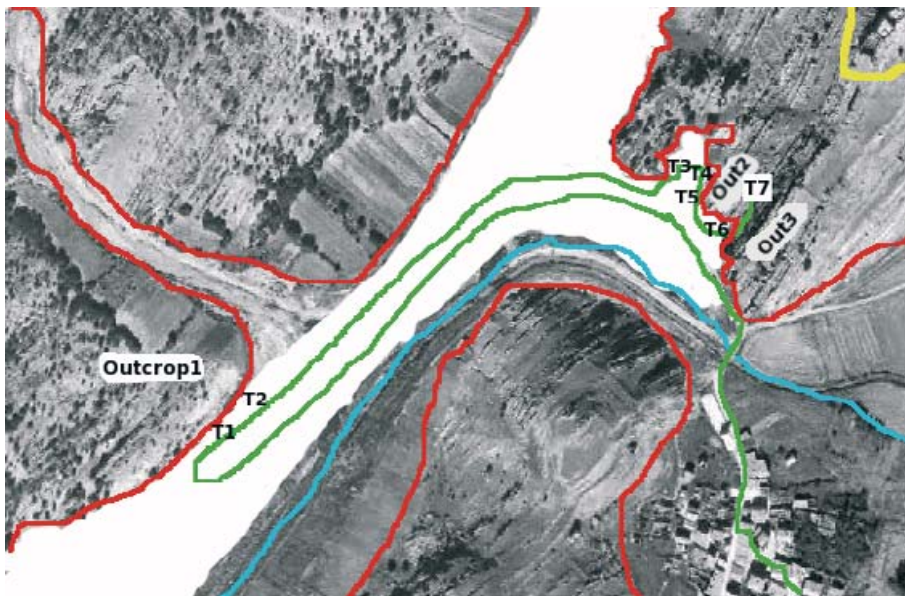


Fig. 4. Map showing the outcrops (Outcrop1, Out2, Out3) and tripod positions (T1–T7) during the Cyborg Astrobiologist mission to Riba de Santiuste in Guadalajara. The village of Riba de Santiuste is shown on the lower right-hand side, and the deserted hilltop castle of Riba de Santiuste is indicated by the yellow outline on the upper right-hand side. The outcrop ‘Outcrop1’ had some strata that were coloured white, as well as a few small 5–10 cm white spots, and a number of iron-oxide concretions. The outcrop ‘Out2’ has a whitish-coloured mineralization near its base. The outcrop ‘Out3’ has alternating layers of red silt-stones and darker-coloured palaeosols. The approximate paths of the river stream are indicated in cyan and the approximate path of our mission is indicated by the green line that goes over the small bridge. The central valley of the image has been coloured white for clarity. The horizontal extent of this aerial photograph is about 1 km.

After segmenting the mosaic image (see Fig. 5), we use a very simple method to find interesting regions in the image: we look for those regions in the image that have a significant number of uncommon pixels. We accomplish this by: first, creating an uncommon map based upon a linear reversal of the segment peak ranking; secondly, adding the three uncommon maps (for *H*, *S*, and *I*) together to form an interest map; and thirdly, blurring this interest map.¹⁰

Based upon the three largest peaks in the blurred/smoothed interest map, the Cyborg system then shows the human operator the locations of these three positions, overlaid on the original image. The human operator can then decide how to use this information; for example whether to ignore the information or to zoom in on one of the interest points. This step can be automated in future versions.

Descriptive summaries of the field site and of the expedition

On 8 February 2005, three of the authors (Díaz-Martínez, Ormó and McGuire) tested the ‘Cyborg Astrobiologist’ system for the second time at a geological site, with red-sandstone layers, near the village of Riba de Santiuste, north of Sigüenza in the northern part of the province of Guadalajara (Spain).

¹⁰ With a Gaussian smoothing kernel of width $B=10$. This smoothing kernel effectively gives more weight to clusters of uncommon pixels, rather than to isolated, rare pixels.

These tests at Riba are meant to be a complementary, confirmatory test of the methodology first tested in the spring of 2004 in Rivas Vaciamadrid. The site in Riba may have more direct relevance as an analogue for the Terra Meridiani site on Mars, which the Mars Exploration Rover, Opportunity, is now exploring. Riba has red-sandstone beds, with some outcrops showing local chemical bleaching due to reduction and mobilization of iron, as well as precipitation of oxidized iron impurities. This process gives the sandstone both dark-red and white-coloured areas. Within the red sandstone, there are concretions of dark-red oxidized iron, as well as some sites where concretion had only been partially complete. Furthermore, the colouring of the red sandstones at Riba is much more ‘brilliant’ and saturated than the unsaturated white colouring of the clay- and sulphate-bearing cliffs in Rivas. The dichotomy and contrast of the colours at Riba, between the oxidized red and the bleached white colours of the sandstones^{11,12,13} certainly made the study of these ‘red beds’ into a relatively

¹¹ Similar imagery and astrobiological hypotheses presented recently by Hofmann (at the *European Astrobiology Network Association (EANA) Conference* in November 2004, at the Open University in Milton Keynes, United Kingdom) inspired us to find such a site in Spain (Hofmann 1990, 2004). Hofmann told one of the authors (McGuire) that there certainly should be several such ‘red bed’ sites in Spain. Later, in December 2004, Díaz-Martínez and McGuire explored several sites in Guadalajara, and found that the site at Riba de Santiuste had some nice red beds, exhibiting the white-bleached areas of red sandstone, which we decided to use for this study.

straightforward, but highly discriminating, test of the Cyborg Astrobiologist's current computer vision capabilities.

The rocks at the outcrops at Riba are of Triassic age (260–200 Myr before present) and consist of sandstones, gravel beds and palaeosols. The rocks were originally deposited during the Triassic in different layers by the changing depositional processes of a braided river system. This river system consisted of active channels with fast transport of sand grains and gravel. During different millenia in the Triassic, the river system shifted and evolved. Therefore, in the example of the palaeosol outcrop, the deposition was only of fine-grained silt, which later was affected by soil processes and formed the palaeosol layers. The rock layers were folded by Alpine tectonics in the Cenozoic.

We arrived at the site at 12 noon on 8 February 2005, and in the next 30 minutes the roboticist quickly assembled the Cyborg Astrobiologist system, and taught the two geologists how to use the system. For the next 4 hours, the two geologists were in charge of the mission, deciding where to point the Cyborg Astrobiologist's camera, interpreting the results from the tablet display, and deciding how to use the Cyborg Astrobiologist's assessment of the interest points in the imagery. Often the geologists chose one of the top three interest points, and then either zoomed in on that point with the zoom lens on the camera, or walked with the camera and tripod to a position closer to the interest point, in order to get a closer look at the interest point with the computer vision system.

The computer was worn on the geologist's belt, and typically took 30 s to acquire and process the image. The images were downsampled in both directions by a factor of 2 during these tests, and the central area was selected by cropping the image; the final image dimensions were 192 × 144.

We chose a set of seven tripod positions at three geological outcrops at Riba de Santiuste in order to test the Cyborg Astrobiologist system (see the map in Fig. 4). This is an improvement upon the number of tripod positions and outcrops

studied in the first mission to Rivas Vaciamadrid in the spring of 2004 (see Table 1). The first geological outcrop at Riba de Santiuste consisted of layered deposits of red sandstone. In several of the images (see Figs 6(a), (b) and (d) for examples), the wearable computer determined aspects of white bleaching to be interesting. Furthermore, in several of the images (see Figs 6(c) and (d) for examples), the wearable computer found the concretions to be interesting. The second geological outcrop was partly covered by a crust of sulphate and carbonate minerals. At this outcrop, the computer vision system found the rough texture of the white-coloured mineral deposits to be interesting (see Fig. 7(a)). At the third geological outcrop, we pointed the camera and computer vision system at a palaeosol. The computer vision system of the wearable computer found the calcified root structures within the palaeosols to be of most interest (see Fig. 7(b)).

Results

Without the problems with shadow and texture that we encountered during our first mission at the white gypsum-bearing cliffs of Rivas Vaciamadrid, the system performed admirably. See Fig. 6(b) for such an example of an image without shadow or texture. We show more details of the automated image processing by the wearable computer of this image in Fig. 5. This image contained an area with bleached domains (in white) in the red sandstone, as well as a few isolated iron-oxide concretions of dark-red colour. Processing this image by image segmentation and by uncommon-map construction was straightforward. The wearable computer reported to the geologists that the three most interesting points were two areas of the white-bleached domain, and a third point in the lower part of the image which was a somewhat darker tone of red. The geologists also found the smaller dark-red concretions in the upper part of the image to be interesting. The wearable computer found these smaller dark-red concretions to be interesting, but only before the interest map was smoothed (or blurred), as summarized in Fig. 5. The wearable computer does not report the top three points from the unblurred interest map to the user. However, the full unblurred interest map, as well as the blurred interest map, are both displayable to the user in real time, and they are both stored to disk for post-mission analysis. We regard the fact that the wearable computer had interest in the dark-red concretions, even though it did not report this interest in its top three interest points, as a partial success. Perhaps, if the camera had zoomed in by a factor of 10, it would have found these dark-red concretions to be interesting, even in the blurred interest map. Hence, these features would be noticed when further approaching the outcrop. Even at this distance, the small size of the dark-red concretions was at the limits of the perception capabilities of the geologists themselves. Nonetheless, the computer did inform the geologists that it had interest in the white-bleached spots and the darker-red region at the bottom of the image, which we regard to be a higher level of success.

¹² Hofmann refers to the white circularly shaped zones where the iron has been first reduced and then removed as 'reduction spheroids'. These spheroids only have a reduced chemical state prior to the removal of the iron, which is mobile when it is reduced. He posits a 'mobile and kinetically inert' biological agent as a possible source of the chemical reduction of the previously oxidized iron. In his studies, the reduced iron is often removed by concentration at the centre of the reduction spheroid. This concentrated iron is later oxidized again, forming a dark-red concretion. Since we only observed a two-dimensional slice (a white disc) through the three-dimensional sphere of the 'reduction spheroid', this may explain why we did not observe any concretions at the centres of the white circles in the red beds at Riba. The concretions at Riba tended to be in a nearby zone that was physically separate from the white zone in the red beds.

¹³ Maybe there have been other concretion-formation mechanisms active at Riba, beyond the model of Hofmann, in which concretions tend to form at the centres of the reduction spheroids. A model, based upon concretion formation in Utah red beds, which includes reducing fluids passing through permeable sandstone beds, has been suggested for the Meridiani haematite deposits on Mars (Chan *et al.* 2004; Ormó *et al.* 2004). In their model, the reducing fluids remove oxidized iron coatings from the sand grains, and later precipitate the iron as spherical concretions when the iron encounters oxidized groundwater.

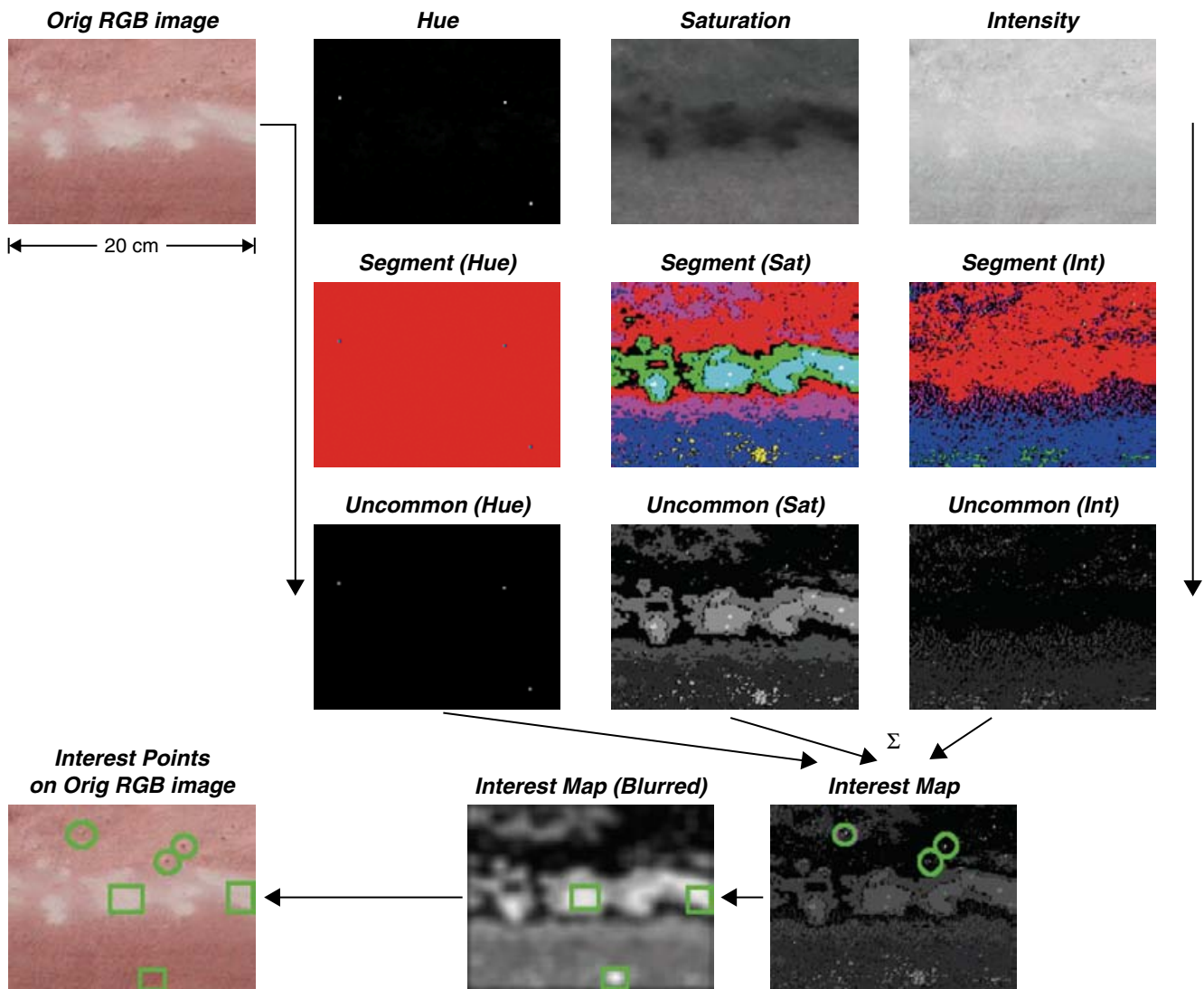


Fig. 5. An image of some white spots and nodules, acquired and processed at tripod position 2 at Riba de Santiuste on 8 February 2005. The wearable computer's autonomous processing of the image is shown, with separate image segmentation and uncommon mapping for each of the hue, saturation and intensity components. The system indicated to the user that the three points indicated by green squares were the most interesting points on a 10 pixel scale. The system also computed that the three points indicated by the green circles were the most interesting points without any spatial summing (on a 1 pixel scale), but it did not indicate this to the user in the field.

In Figs 6 and 7, we present a number of other images that were acquired and processed by the Cyborg Astrobiologist at Riba de Santiuste. For each image, we show here the image segmentation for the saturation slice of the colour image, since the saturation slice discriminated the red and white colours rather well. We also show the final, blurred interest map, which was computed by summing the uncommon maps for hue, saturation and intensity as in Fig. 5, and then smoothing the resulting map. Figure 6(a) shows the border between a large oxidized red-coloured zone of the red bed and a large bleached white-coloured zone of the red bed. The wearable computer found the texture in the white zone to be most interesting. Figure 6(c) shows a highly magnified view of some of the concretions in the red bed near tripod position 2. These concretions are not well rounded like 'blueberries'; rather, they are more like the 'popcorn'

concretions observed by Opportunity at Meridiani Planum. The computer vision system in the wearable computer found two of the darker-red concretions on the left-hand side of the image to be interesting, and one bright white area on the right side of Fig. 6(c) to be interesting. The discriminatory power of the image segmentation was not very clean at this high level of magnification. Figure 6(d) shows a zoomed-out view of some concretions and a bleached white zone near tripod position 2. The computer vision system found the area of the concretions to be most interesting, followed by the bleached area in the left-hand side of the image. As shown in Fig. 6(e), in the same part of the outcrop were some quartzite rocks of green, grey and yellow colours. In an image containing these rocks, the computer vision system found several of them to be more interesting than the surrounding red sandstone.

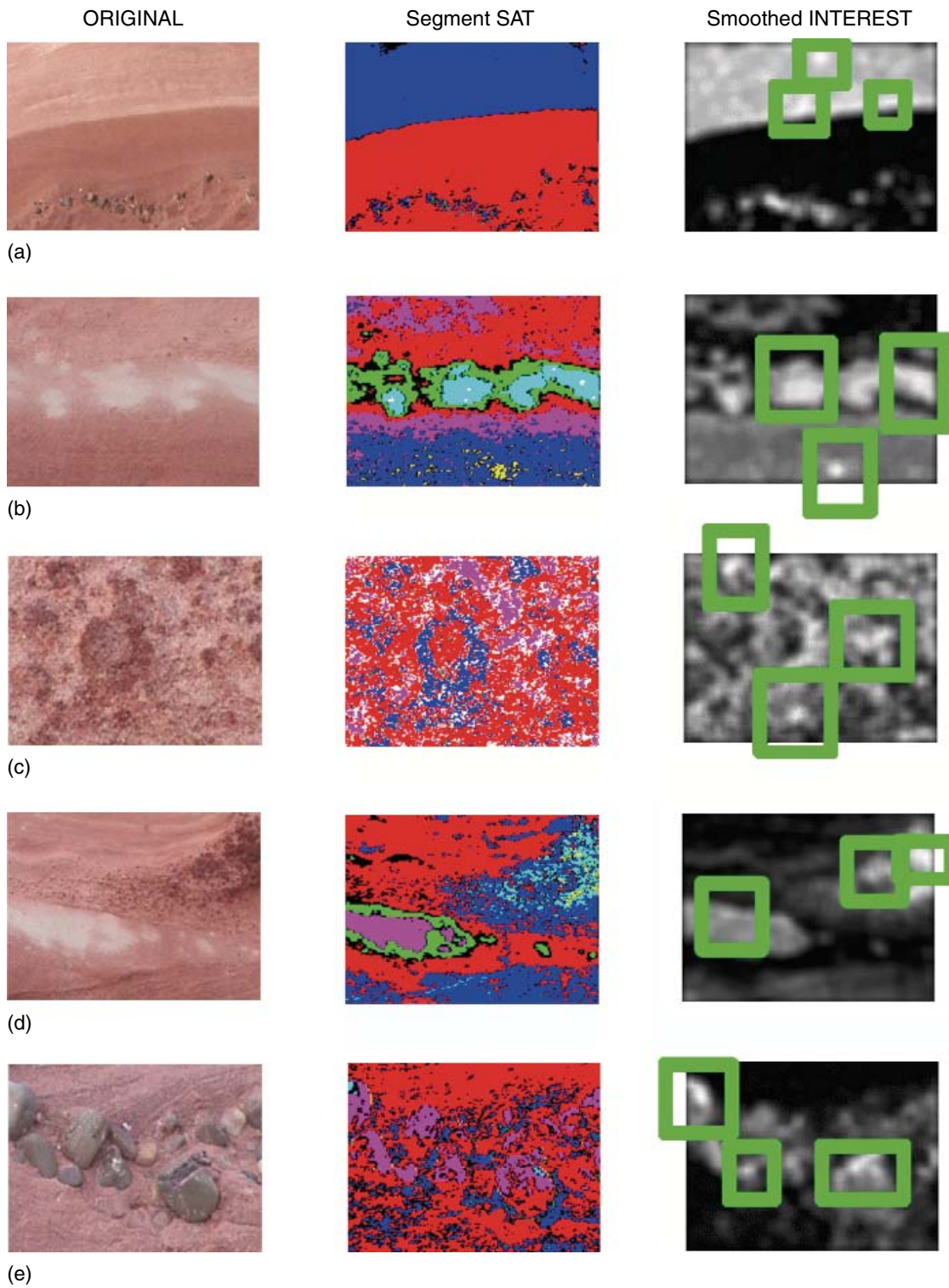


Fig. 6. Some examples of various images, their image segmentations (for saturation), their interest maps and their top three interest points. These images were acquired and processed at tripod positions 1 and 2, near outcrop 1.

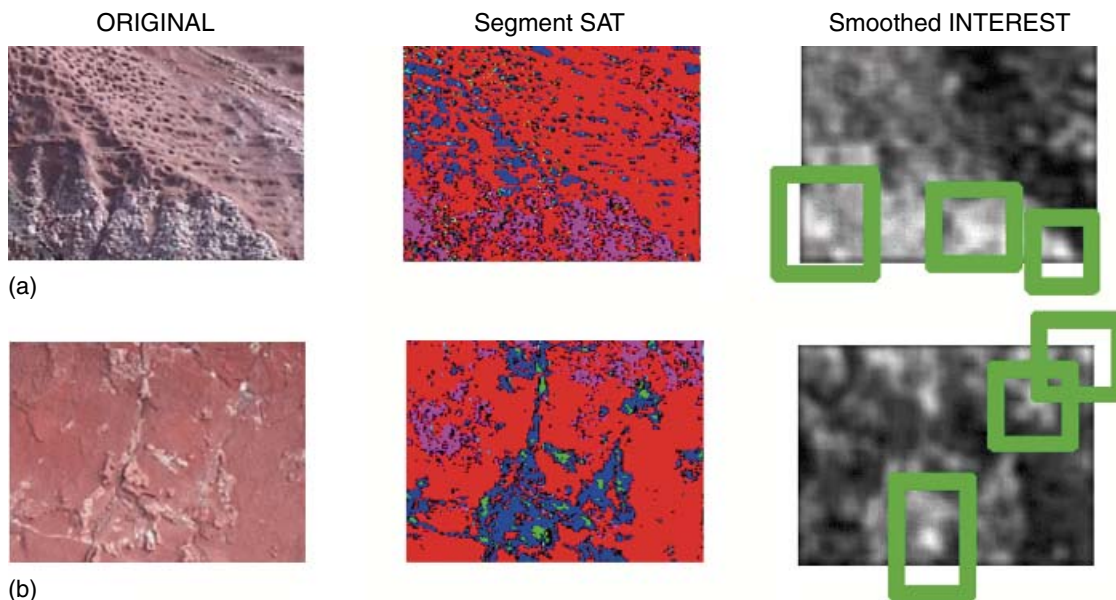


Fig. 7. Some examples of various images, their image segmentations (for saturation), their interest maps, and their top three interest points. These images were acquired and processed at tripod positions 4 and 6, near outcrops 2 and 3.

Likewise, at the second outcrop, we observed some highly textured mineral deposits of whitish colours. In a zoomed-out view of these mineral deposits (Fig. 7(a)), the wearable computer found the texture of the mineral deposits to be more interesting than the more homogenous red colour of the neighbouring sandstone.¹⁴ The wearable computer did not find the highly textured region containing many dark holes to be as interesting as the white-textured mineral deposits. In an ideal computer vision system, one of the top three interest points probably should have been within the region with all of the dark holes. These dark holes formed by a combination of physical (wind erosion) and chemical (differential cementation) processes.¹⁵ Based partly upon the guidance of the wearable computer, we acquired several samples of the mineral deposits for analysis in the laboratory. Based upon the

¹⁴ The software of the Cyborg Astrobiologist has not been configured to segment the images into different regions, based upon the texture of each different region. The software only uses grey-level differences for the image segmentation, but for each of the three different colour layers. However, when there is a significant amount of variation of the grey-levels within a region (which is often caused by texture), then the software will probably label many of the pixels in that region as being uncommon. Therefore, our system does have some capabilities to study texture.

¹⁵ The current Cyborg Astrobiologist system certainly is biased towards colour or intensity differences over differences in physical morphology. Our system uses colour properties, and not morphology to make its decisions. In geological samples, the colour differences are often a result of differences in chemistry (i.e. differences in the chemical composition, the state of oxidation of iron, etc.). Furthermore, in geological samples, the differences in physical morphology also depend on chemistry (erodability, which in turn depends on differential cementation, etc.), but mostly on the geometry of internal structures, their size, spacing, etc. Certainly, adding morphology as a layer in the interest map would be very beneficial to our system.

geologists' experience and upon acid tests of these mineral deposits at the field site, we suspected that the mineral deposits consisted largely of a white textured overlayer of 15–20 mm of a sulphate, with a thin grey underlayer of 1–10 mm of calcite. The laboratory tests later confirmed that the overlayer is largely composed of hydrated calcium sulphate (gypsum).

At the third outcrop, the Cyborg Astrobiologist system studied a layer of palaeosols, which are 'affected' silty deposits from a fluvial plain.¹⁶ These palaeosols contained partly calcified root structures of plants that grew in this fluvial plain during the Triassic. At tripod position 6, our computer vision system found the white-coloured calcified root structures to be more interesting than the surrounding matrix of red siltstone (Fig. 7(b)). However, at tripod position 7, in a more complex image (not shown here) with more root structures and more diverse colouring, the computer vision system did not find the root structures to be particularly interesting.¹⁷

¹⁶ 'Palaeosol' is the series of features (colour, structures, layers, minerals, etc.) which indicate that the sediment was affected by *soil processes* in the past. Such soil processes include leaching, oxidation, reduction and precipitation.

¹⁷ At tripod position 6, the system worked much better because the root structures were a sufficiently minor component of the image; the reddish-coloured parts of the palaeosol dominated. At tripod position 7, the system did not work well because the root structures covered an area in the image that was greater than the areas of some of the other minor components of the image. In future enhancements of the computer vision system, if root structures are deemed by the mission scientists to be of sufficient interest, then we could develop an interest-map algorithm that would respond to webs of linear connected features such as root structures, or we could develop a different interest-map algorithm which could be biased towards whitish-coloured areas which are unlike all the other colours of the mostly reddish palaeosols.

We have compared the Cyborg Astrobiologist's performance in picking the top three interest points with a human geologist's quasi-blind classification. Geologist Díaz-Martínez verbally noted the interesting parts of the image. Then he was shown the Cyborg Astrobiologist's top three interest points; he then judged how well the computer vision system matched his own image analysis. We judged that there was concurrence between the human geologist and the Cyborg Astrobiologist on the interest points about 69 times (true positives), with 32 false positives and with 32 false negatives, for a total of 32 images studied. This was an average of 2.1 true positives (TP) for each image out of a possible (usually) three trials per image; an average of 1.0 false positive (FP) per image out of a possible (usually) three trials per image; and an average of 1.0 false negatives (FN) per image, with no *a priori* limitation on the number of false negatives per image. There was double counting of positives since sometimes a localized physical feature corresponded to more than one interesting features in the image (i.e. one image had some parallel lines at a geological contact, so the interest points corresponding to this region counted doubly). One way to look at this data is to take the ratios $tpr = TP / (FP + TP)$, $fpr = FP / (FP + TP)$ and $fnr = FN / (FP + TP)$. With our technique, it is difficult to assess the true-negative rate tnr . For the data from Riba, we compute: a true-positive rate of $tpr = 68\%$, a false-positive rate of $fpr = 32\%$ and a false-negative rate of $fnr = 32\%$. We did not attempt to compute the receiver operating characteristic (ROC) curves for these images, as a function of the number of interest points computed for each image. A more careful analysis could be made with many more images from different field sites, but these numbers agree qualitatively with the results we were getting at Rivas Vaciamadrid, even though we have not computed the statistics. Qualitatively, we expect that for the types of imagery that we typically study, the Cyborg Astrobiologist will not do a near-perfect job (with the geologist-concurrence analysis giving fpr and fnr both less than 10%), nor will it do a poor job (with the geologist-concurrence analysis giving either or both fpr and fnr greater than 90%), it typically has mid-level false-positive and false-negative rates – a mid-level in performance. Of course, we would like to improve the system to do a near-perfect job, but considering the simplicity of the image-segmentation algorithm and the uncommon-mapping technique, we believe that this work can provide a good basis for further studies.

One approach for improving the false-positive rate is to include further filtering of the interest points that are currently being determined from the uncommon maps. In that way, errant positives could be caught before they are reported to the human operator. Right now in the field, the human operator serves as a decent filter of false positives, so fixing the false-positive rate is not so urgent; fixing the false-negative rate is somewhat more important. One approach for improving the false-negative rate would be to compute interest features in new and different ways (i.e. with edge detectors or parallel-line detectors), in order to ensure that all of the interesting features are detected. Both approaches could be

attacked, for example, by using context-dependent geologist knowledge, which would need to be coded into a future, more advanced Cyborg Astrobiologist. Currently, considering that we do not deploy such context-dependent geologist knowledge, our relatively unbiased uncommon-mapping technique seems to be doing rather well.

Discussion and conclusions

We have shown that our Cyborg Astrobiologist exploration system performs reasonably well at a second geological field site. Given similar performance at the first geological field site, we can have some degree of confidence in the general unbiased approach towards autonomous exploration that we are now using. We can also have sufficient confidence in our general technique that we can use our specific technique of image segmentation and uncommon mapping as a basis for further algorithm development and testing.

In the near future, we plan to:

- upgrade our image-segmentation algorithm, in order to handle texture and colour simultaneously (cf. Freixenet *et al.* 2004); this upgrade may give us more capabilities to handle shadow as well;
- test the Cyborg Astrobiologist system at field sites with a microscopic imager; this will complete our mimicry of a stepwise approach by a human geologist towards an outcrop.

At Riba de Santiuste, our system has been tested for exploration on imagery at a site that is not unlike Meridiani Planum, where the MER Opportunity is now exploring. Riba de Santiuste is similar to Meridiani Planum in its iron-oxide concretions and its sulphate mineral deposits. The bleached-white zones of the red sandstones at Riba de Santiuste may be an analogue for similar geochemical or perhaps biological phenomena on Mars (Hofmann 1990, 2004; Chan *et al.* 2004; Ormó *et al.* 2004). The software behind the Cyborg Astrobiologist's computer vision system has shown its initial capabilities for imagery of this type, as well as for imagery of some other types. This computer vision software may one day be mature enough for transplanting into the computer vision exploration system of a Mars-bound orbiter, robot or astronaut.

Acknowledgements

P. McGuire, J. Ormó and E. Díaz-Martínez would all like to thank the Ramon y Cajal Fellowship programme of the Spanish Ministry of Education and Science. Many colleagues have made this project possible through their technical assistance, administrative assistance or scientific conversations. We give special thanks to Kai Neuffer, Antonino Giaquinta, Fernando Camps Martínez and Alain Lepinette Malvitte for their technical support. We are indebted to Gloria Gallego, Carmen González, Ramon Fernández, Coronel Angel Santamaria and Juan Pérez Mercader for their administrative support. We acknowledge conversations with Beda Hofmann, Virginia Souza-Egipsy, María Paz Zorzano

Mier, Carmen Córdoba Jabonero, Josefina Torres Redondo, Víctor R. Ruiz, Irene Schneider, Carol Stoker, Jörg Walter, Claudia Noelker, Gunther Heidemann, Robert Rae, Jonathan Lunine, Ralph Lorenz, Goro Komatsu, Nick Woolf, Steve Mojzsis, David P. Miller, Bradley Joliff, Raymond Arvidson and Daphne Stoner. The field work by J. Ormö was partially supported by grants from the Spanish Ministry of Education and Science (AYA2003-01203 and CGL2004-03215). The equipment used in this work was purchased by grants to our Center for Astrobiology from its sponsoring research organizations, CSIC and INTA.

References

- Chan, M.A., Beitley, B., Parry, W.T., Ormö, J. & Komatsu, G. (2004). A possible terrestrial analogue for haematite concretions on Mars. *Nature* **429**, 731–734.
- Compton, W.D. (1989). *Where No Man Has Gone Before: a History of Apollo Lunar Exploration Missions*, chs 13–14. Based on NASA History Series SP-4214. <http://www.apolloexplorer.co.uk/default.asp?libsrc=/books/sp-4214/cover.htm>, <http://www.hq.nasa.gov/office/pao/History/SP-4214/card.html>, <http://www.hq.nasa.gov/office/pao/History/SP-4214/contents.html>
- Freixenet, J., Muñoz, X., Martí, J. & Lladó, X. (2004). Color texture segmentation by region–boundary cooperation. In *Computer Vision, ECCV 2004, 8th European Conf. on Computer Vision, Proc., Part II (Lecture Notes in Computer Science*, vol. 3022), ed. Pajdla, T. & Matas, J., pp. 250–261. Springer, Prague. Also available in the *CVonline* archive: http://homepages.inf.ed.ac.uk/rbf/CVonline/LOCAL_COPIES/FREIXENET1/eccv04.html
- Haddon, J.F. & Boyce, J.F. (1990). Image segmentation by unifying region and boundary information. *IEEE Trans. Pattern Anal. Mach. Intell.* **12**(10), 929–948.
- Haralick, R.M., Shanmugan, K. & Dinstein, I. (1973). Texture features for image classification. *IEEE SMC-3*(6), 610–621.
- Hofmann, B. (1990). Reduction spheroids from northern Switzerland: mineralogy, geochemistry and genetic models. *Chem. Geol.* **81**, 55–81.
- Hofmann, B. (2004). Redox boundaries on Mars as sites of microbial activity. In *IV European Workshop on Exo/Astrobiology*, held at the Open University, Milton Keynes, abstract, [http://physics.open.ac.uk/eana/TALKS/Redox boundaries on Mars as sites of microbial activity.pdf](http://physics.open.ac.uk/eana/TALKS/Redox%20boundaries%20on%20Mars%20as%20sites%20of%20microbial%20activity.pdf)
- McGuire, P.C. *et al.* (2004a). Cyborg systems as platforms for computer-vision algorithm-development for astrobiology. In *Proc. III European Workshop on Exo/Astrobiology, Madrid, European Space Agency Special Publication, ESA SP-545*, pp. 141–144. <http://arxiv.org/abs/cs.CV/0401004>, http://www.adsabs.harvard.edu/cgi-bin/nph-bib_query?bibcode=2004eab.conf..141m&db_key=AST&data_type=HTML&format=&high=42ad60865b01644
- McGuire, P.C., Ormö, J.O., Díaz-Martínez, E., Rodríguez-Manfredi, J.A., Gómez-Elvira, J., Ritter, H., Oesker, M. & Ontrup, J. (2004b). The Cyborg Astrobiologist: first field experience. *Int. J. Astrobiol.* **3**(3), 189–207. <http://arxiv.org/abs/cs.CV/0410071>
- Ormö, J., Komatsu, G., Chan, M.A., Beitley, B. and Parry, W.T. (2004). Geological features indicative of processes related to the hematite formation in Meridiani Planum and Aram Chaos, Mars: a comparison with diagenetic hematite deposits in southern Utah, USA. *Icarus* **171**, 295–316.
- Ritter, H. *et al.* (1992, 2002). The Graphical Simulation Toolkit, Neo/NST. http://www.techfak.uni-bielefeld.de/ags/ni/projects/neo/neo_e.html
- Schmitt, H.H. (1987). A field geologist's return to the moon. In *Abstracts of the Lunar and Planetary Science Conf. XVIII*, vol. 18, pp. 880–881.
- Scott, J.R., McJunkin, T.R. and Tremblay, P.L. (2003). Automated analysis of mass spectral data using fuzzy logic classification. *J. Assoc. Lab. Automat.* **8**(2), 61–63.
- Scott, J.R. & Tremblay, P.L. (2002). Highly reproducible laser beam scanning device for an internal source laser desorption microprobe Fourier transform mass spectrometer. *Rev. Sci. Instrum.* **73**(3), 1108–1116.
- Squyres, S. *et al.* (2004). *In situ* evidence for an ancient aqueous environment at Meridiani Planum, Mars. *Science* **306**, 1709–1723.